Rock mass change monitoring in a sill pillar at Vale's Coleman mine (Sudbury, Canada)

Benoît Valley
Geomechanics Research Centre, MIRARCO – Mining Innovation, Sudbury, ON, Canada
Centre for Excellence in Mining Innovation - CEMI, Sudbury, ON, Canada
Bernd Milkereit, Winnie Pun
Department of Physics, University of Toronto, Canada
Marco Pilz
GFZ German Research Centre for Geosciences
Jean Hutchinson, Dani Delaloye
Department of Geological Sciences and Geological Engineering, Queen's University, Kingston, Canada
Behrad M. Madjdabadi
Department of Civil Engineering, University of Waterloo, Waterloo, Canada
Maurice Dusseault
Department of Earth and Environmental Sciences, University of Waterloo, Waterloo, Canada
Denis Thibodeau and Anneta Forsythe
Vale, Sudbury, Canada

ABSTRACT: Optimization of the mining sequence in terms of economics (maximizing net present value) often leads to multi-front mining methods generating pillars. Significant resources are tied up in these pillars, but mining them is often challenging. In order to improve our understanding of rock mass behaviour while extracting these pillars, an extensive monitoring program has been designed and implemented at Vale's Coleman mine (Sudbury, Canada). The program focuses on existing and new technologies that have potential for monitoring deformation and rock mass property changes. It includes both active and passive methods: gravimeters, multi-point borehole extensometers, fiber optic strain meters, fixed and portable three-component seismic arrays, borehole imaging and sonic logging, and, repeated LiDAR surveys. This paper reports results from an initial project phase, when only a small amount of mining has taken place. The goal was to test and compare technologies in order to assess their sensitivity, accuracy, repeatability and suitability for underground mining conditions. Value is gained by having a broad range of monitoring devices running side by side, enabling comparisons and benchmarking.

1 INTRODUCTION

Significant developments in monitoring technologies have occurred in recent years. Monitoring devices are now smaller, powered by battery, and communicate wirelessly, enabling their deployment in denser arrays. New technologies have also been developed, including high resolution laser scanning (LiDAR) and fiber optic strain monitoring. Combining multiple systems provides information on rock mass deformation and rock mass failure processes occurring over a range of frequency and spatial scales. The potential of these technologies to better monitor rock mass response while mining is large; however, bringing new technologies into an industry also comes with challenges. Before a new technique can be accepted, proof of concept, benchmarking with existing technology and reliability assessment are needed. The goal of the study reported herein is the development and implementation of new technologies for monitoring in deep underground mines. It capitalises on an opportunity presented at Vale's Coleman mine (Sudbury, Ontario), where it was possible to install a dense monitoring array in a sill pillar that is currently being extracted. A particular focus of this work is on monitoring techniques with potential for rock mass change monitoring using continuous or time lapse approaches.

2 FIELD TESTING CONTEXT

The field test context is shown in Fig. 1. The current mining situation is the early stage of extraction of a 25 m high sill pillar (Fig. 1a). Top sill and bottom sill development give access to the mining area (Fig. 1c). An array of monitoring holes was drilled from the top sill level. A subset of the holes drilled for the project, from which results are presented in this paper, is shown in Fig. 1b & c (numbered 1 to 5). The collection of field data took place mostly during the time interval 3rd to 6th of June, 2011. At the time, stope A in Fig. 1b & c was the only actively mined stope. Some data collection, for example the borehole deformation data, continued over a longer time frame during which stopes A to E were actively mined.

3 DATA COLLECTION AND ANALYSES

3.1 Borehole imagery

Borehole imagery was collected in the monitoring holes for two purposes: 1) to provide general rock mass characterisation data; and 2) to evaluate the suitability of borehole imagery for monitoring changes. An optical televiewer (OBI40 from ALT)[1] and an acoustic televiewer (ABI40 from ALT) were tested. The logs were acquired in 4 inch (101 mm) diameter, percussion-drilled holes.

The quality of the acquired logs was generally good despite the fact that the boreholes were percussively drilled (rough walls). The optical images were clear and details of the rock texture could be evaluated. Open joints are easily seen on the acoustic amplitude image. The wall roughness is clearly visible on the amplitude image, but it doesn't significantly affect the ability to identify features on the amplitude image or the proper identification of travel time.

Examples of parameters influencing optical image quality are shown in Fig. 2. Good probe centralisation using stiff centralisers is critical; poor centralisation results in shading of the image (Fig. 2a & b). A comparison between a log from a dry hole and one taken in the same hole after filling it with clear water is shown in Fig. 2c & d. The water influences the recorded image; in this case it increases the image contrast. These examples indicate that strict control of the logging conditions is necessary to get images that can be evaluated for monitoring changes if repeated logging data are acquired over time.

Two repeatability tests of the acoustic televiewer have been performed. The first, presented in Fig. 3, consisted of recording data while keeping the probe at a fixed depth (Fig. 3a & b). This way the

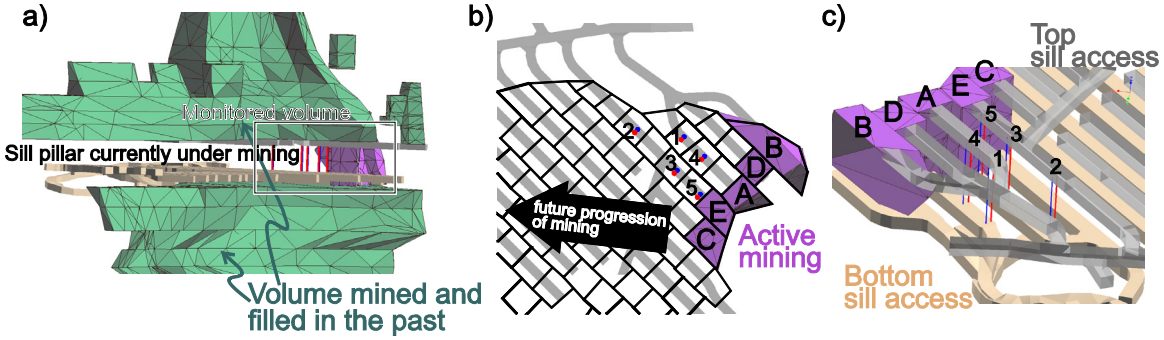

Figure 1: Overall geometry of the monitored volume a) Isometric view of the broader mining context (pillar thickness is about 25 m) b) plan view of the monitored area (typical stope size: 15m x 15 m). c) Isometric view of the monitored volume. Red: monitoring hole with fibre optic sensing cables and blue: monitoring holes with multi-point borehole extensometer.

[1] Use of brand names does not imply a recommendation for a particular product.

repeatability of the probe components (transducer, electronic) can be tested without the influence of geometry (probe repositioning in the hole). For all data plots together for amplitude (Fig. 3c) and travel time (Fig. 3d, displayed here in polar coordinates to look similar to a borehole section) it is evident that the repeatability is generally good, i.e. all curves are closely overlapping. The variations of the recordings relative to the first reading confirm this impression with variations of less than 5% for the amplitude (Fig. 3e) and less than 1% for the travel time (Fig. 3f). The second test presented in Fig. 4 considered a comparison of repeated logging of the same section on the same day, thus no rock mass changes were expected. Repeatability is better for the travel time than for the amplitude data but is generally good for both log types. The presence of fractures locally influences the repeatability.

3.2 Sonic logging

As with the televiewer data, full waveform sonic (FWS) data acquired with a triple receiver Mount Sopris probe is evaluated for repeatability. Two cases are considered: 1) static, i.e. repeated measurement at a fixed position, and 2) repeated logging, i.e. running the probe twice in the same borehole.

For the static recording, repeated measurements are very similar with the waveforms overlapping almost perfectly (Fig. 5a). The cross correlation method (CC) is used to test the resemblance of the signals. One example is presented in Fig. 5b which suggests good repeatability since the CC function almost replicates an autocorrelation function (symmetric about zero lag). Maximum cross-correlation coefficient

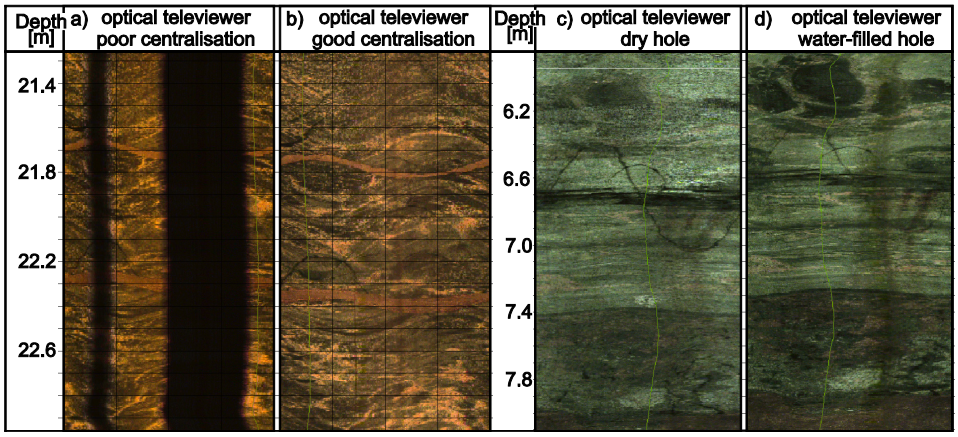

Figure 2: Repeated optical televiewer image illustrating the influence on image quality of a), b) tool centralisation and c), d) water conditions.

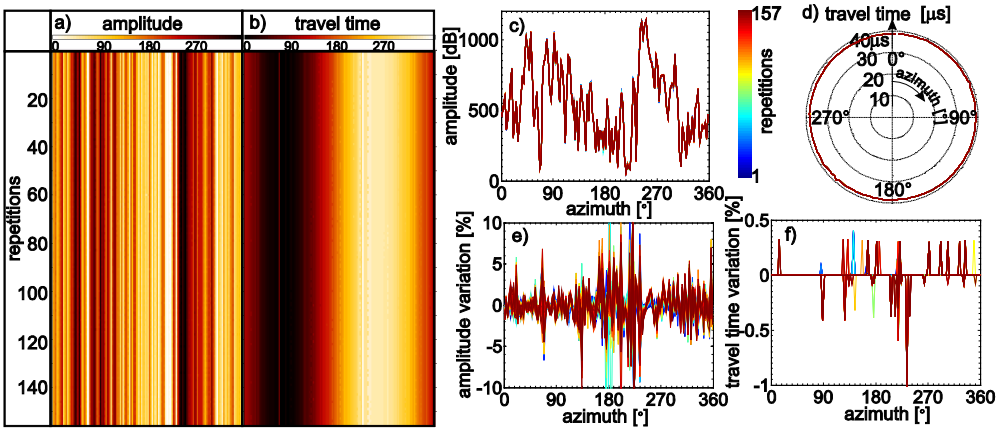

Figure 3: Acoustic televiewer repeatability test a) and b) static logs for amplitude and travel time respectively. c) to e) test of repeatability (see text for details).

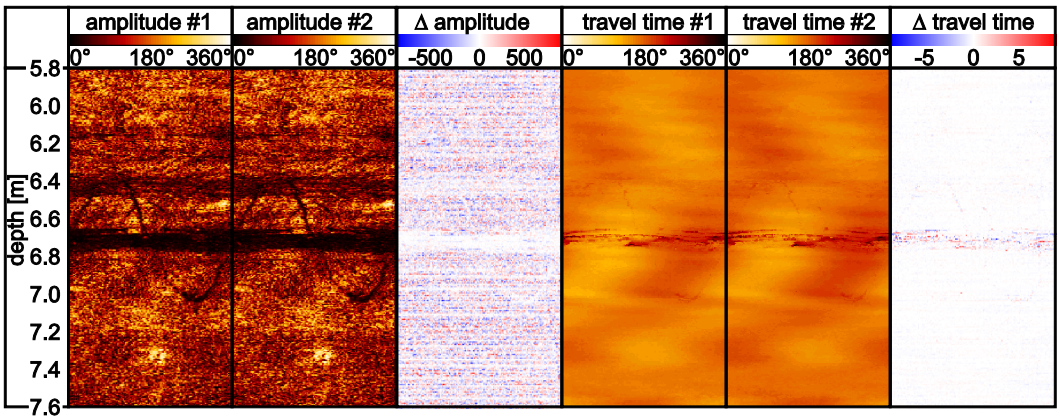

Figure 4: Comparison of repeated logs (#1 and #2) acquired on the same day (no rock mass change expected).

and its corresponding lag are extracted for each repetition (Fig. 5c). The results always showed zero lag, which indicates that the transmitter of the sonic probe is stable and repeatable.

Similarly, data were compared from two repeated logs. Waveforms from the same depth are visually less similar than for the static case (Fig. 5d), and there is some non-symmetry in the CC function (Fig. 5e), but the maximum CC coefficient still occurs at zero lag. This is the case for most of the trace except for the intervals 9 to 11 m and 12 to 14 m. These zones correspond to fractured zones.

3.3 Borehole deformation monitoring

Two systems were deployed to monitor rock mass deformation: 1) multipoint borehole extensometers (MPBX) and 2) fiber optic strain monitoring devices. The latter is a new type of deformation monitoring device developed originally for structural and civil applications (e.g. pipeline, bridges, dams monitoring). It has the potential for both high sensitivity and high spatial resolution. Details of the technology are given in Thévenaz (2010). It uses the temperature and strain dependency of the Brillouin frequency shift, a property of scattered light travelling in a fibre under specific conditions. By using

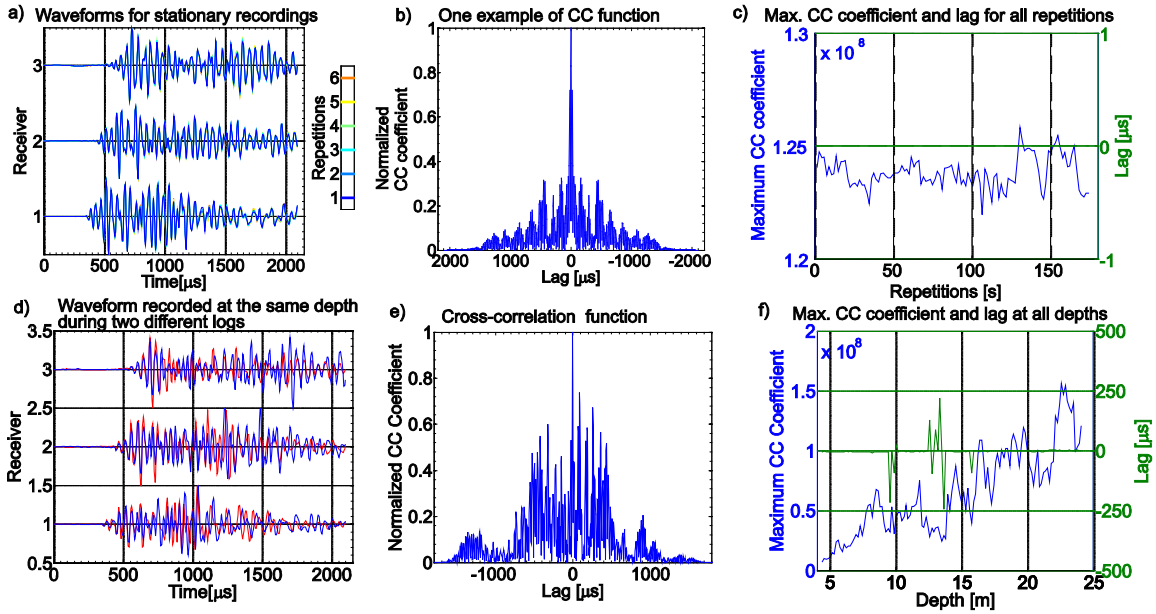

Figure 5: Repeatability test for static recording (a to c) and repeated logging (d to f).

reflectometry, the distance along the sensing fibre is obtained by processing the data initially collected in the time domain.

Both systems were installed in parallel holes (see Fig. 1) to provide an opportunity to benchmark the fibre optic system. The results from hole #1 of Fig. 1 are presented in Fig. 6. The deformation profiles from both systems are qualitatively similar, however, the high spatial resolution of the fibre optic system allows us to determine that the deformation has taken place precisely on a fracture that is visible on the optical televiewer image of that hole (Fig. 6c). The limited number of anchors of the MPBX does not permit such a precise interpretation. However, the fibre system is affected by a cyclic noise with a wavelength of about 1.3 m. This noise is attributed to the manufacturing process of the sensor (Valley *et al.*, 2012). There is also a disagreement in the deformation magnitude measured by both systems: the MPBX measured deformation is about 5 times larger than the deformation readings from the fibre system. This is attributed to a different strain transfer ratio related to the rock/grout/sensor compliance contrast (Madjdabadi et al., 2012), i.e. the borehole filling and cable sensor being much softer than the rock around it, only a fraction of the deformation encountered by the rock is transmitted to the sensor. In addition, de-bonding and slippage at the sensor/grout interface is not excluded.

3.4 Drift deformation monitoring using LiDAR

Another attempt to measure the rock mass deformation was made by taking repeated scans of the bottom sill drifts walls using LiDAR. LiDAR is a remote sensing technology that produces a high resolution, high accuracy 3D point cloud (e.g. Lato, 2010), where each point as positional data (x,y,z) and an intensity return (i). The LiDAR system used here is a Leica HDS6000 that allows scan acquisition at a rate of 508,000 points/s at a positional accuracy of about 5 mm (single scan point accuracy). For a face located 10 m away from the LiDAR scanner, a grid with a resolution of 1.6 x 1.6 mm is acquired, and a smaller point spacing can be acquired for a face located closer or if a higher scan resolution is used. Multiple scans were aligned in order to obtain complete, high resolution coverage of the area of interest. Two successive scanning programs were completed, the first one on May 18/19, 2011 and the second one on Sep-15, 2011. Stope A (see Fig. 1) was actively mined during the first scan. Stope B was mined and filled in the interim and stope C was being actively mined when the second scan was acquired.

A photograph of the acquisition setup is presented in Fig. 7a and the acquired data point cloud at the same location is presented in Fig. 7b. The image of the scan illustrates the decrease in resolution with increasing distance from the scanner. Fig. 7c shows a detailed view of a section of the acquired data. Very fine details including bolt plates, mesh and cables are clearly captured in the scan. By aligning multiple scans, high resolution datasets for the entire area of interest are obtained.

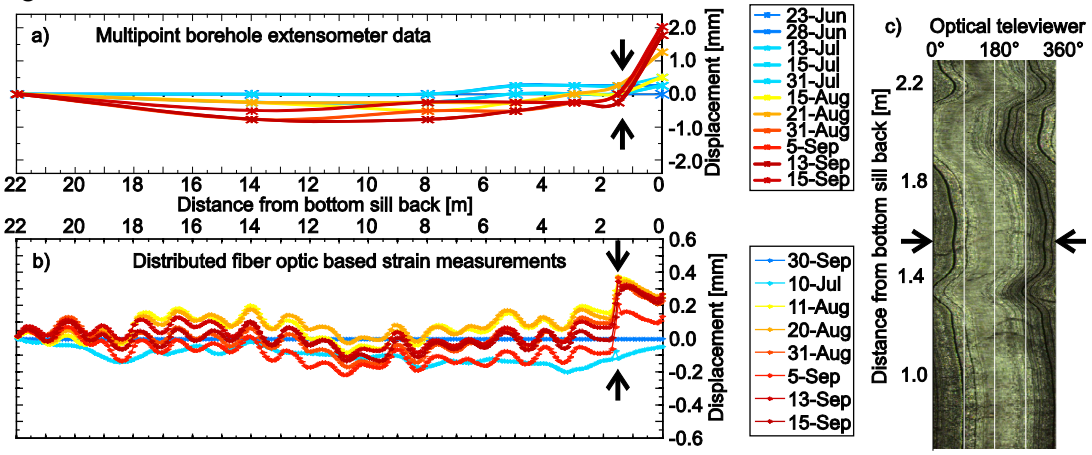

Figure 6: comparison of deformation profiles acquired with a MPBX system (a) and a fibre optic system (b). Most of the deformation occurs at a fracture visible on the optical televiewer image (c).

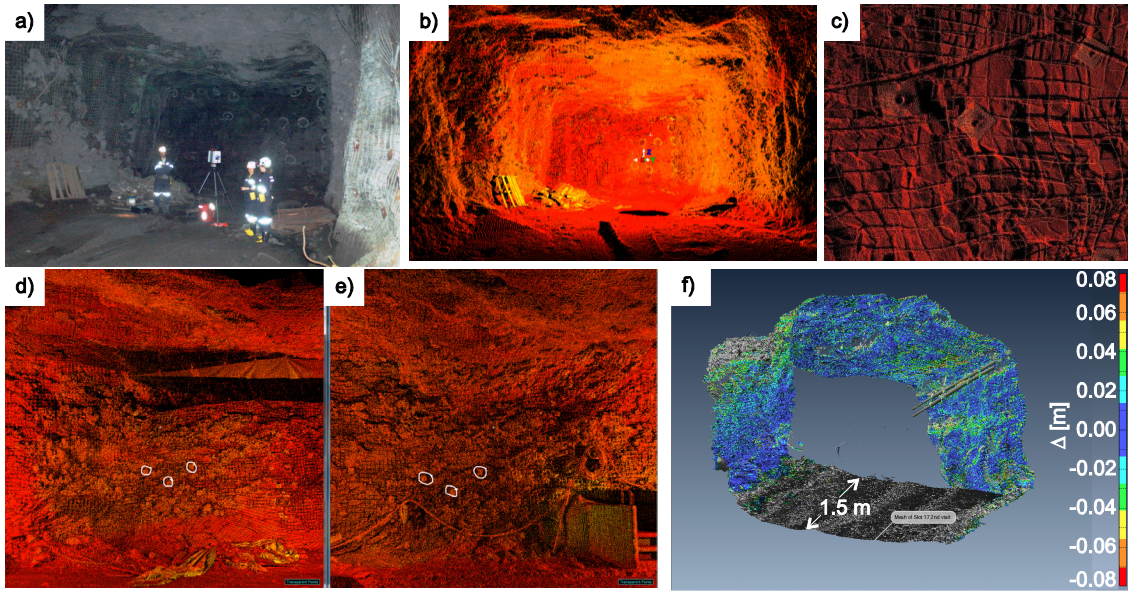

Figure 7: a) LiDAR data acquisition setup and b) LiDAR point cloud. c) details of LiDAR data. d) and e) present two data set acquired on the same drift wall at 4 months interval. f) difference image generated by comparing successive scans.

An attempt to use these LiDAR datasets for change monitoring is presented in Fig. 7d to f. Two scans of the same drift wall acquired at a 4 month interval are presented in Fig. 7d & e. Common features such as bolt plates (circled in white on the Figure) can be identified in both scans. By using the common features to align the two temporal scans then computing the shortest distance between points in successive scans, a changes image can be generated. Such an image is presented in Fig. 7f. Research is in progress to identify rock mass deformation and determine the accuracy and scale of change measurement possible with LiDAR scanning (Delaloye et al., 2012).

3.5 Seismic monitoring

Advanced seismic data acquisition and processing were performed in order to obtain seismic information within a much broader frequency range than typically done in underground hard rock mines. Three seismic systems were run in parallel: 1) an ESG micro-seismic system including triaxial and uniaxial accelerometers, 2) a GFZ-WISE wireless seismic array (Picozzi *et al*., 2010) including geophone sensors with an Eigen frequency of 4.5 Hz, and 3) a high-sensitivity Micro-g LaCoste gravimeter. The combination of these systems allowed a frequency coverage of more than 8 order of magnitudes (see Fig. 8). Such a broad band coverage permitted identification of activities that are not typically considered in mine seismic monitoring, including (see Fig. 8) earth tides, global seismic events and tremors. Due to the continuous acquisition of the data it is further possible to study changes in the frequency content of the seismic noise signals due to changes in local site conditions.

In global seismology, non-volcanic tremors show dramatic differences in waveform and source spectra which suggests distinct physical processes for tremors versus local seismic events (Kao et al., 2005). In this experiment, tremors are identified in the recorded signal by performing autocorrelation analyses. An example of a data set containing tremor and a seismic event is presented in Fig. 9. The tremor central frequency is 28 Hz. With the available data, it is not possible to identify if the source of the tremor was due to geomechanical effects (stress redistribution...) or if it was induced by other sources. It cannot be excluded that such signals are induced by mechanical equipment (e.g. pumps). Indeed, it has been documented in oilsands operations that on-board motors and pumps of mining equipment running at 1750

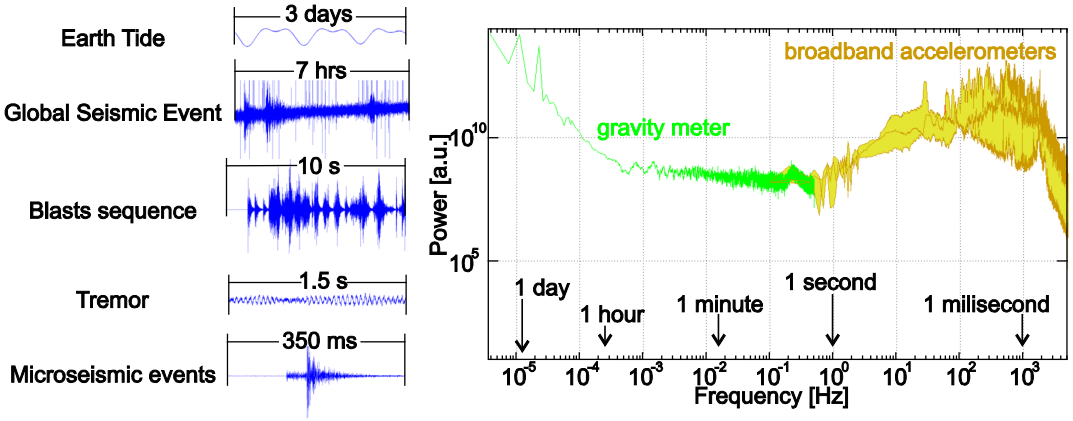

Figure 8: Combination of seismic systems allowed the acquisition of data over a frequency range of more than 8 order of magnitude.

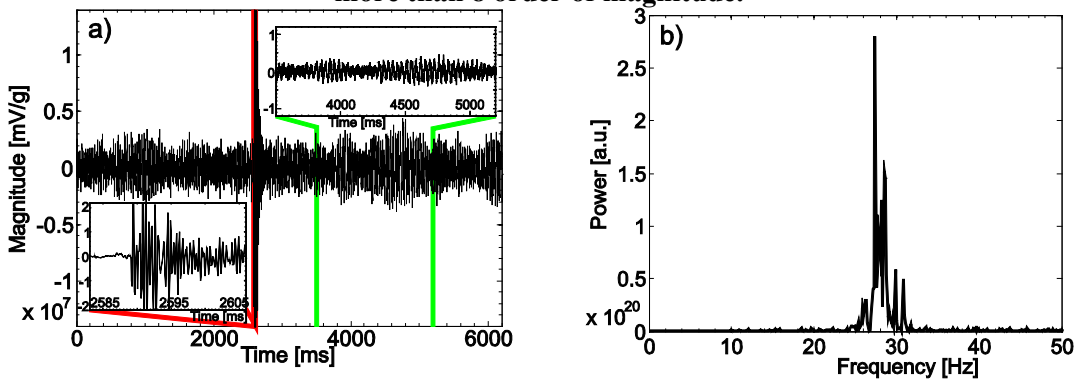

Figure 9: a) Example of seismic data set containing both a microseismic event (lower left insert) and a tremor (upper right insert). b) power spectrum of the tremor signal showing a central frequency of 28 Hz.

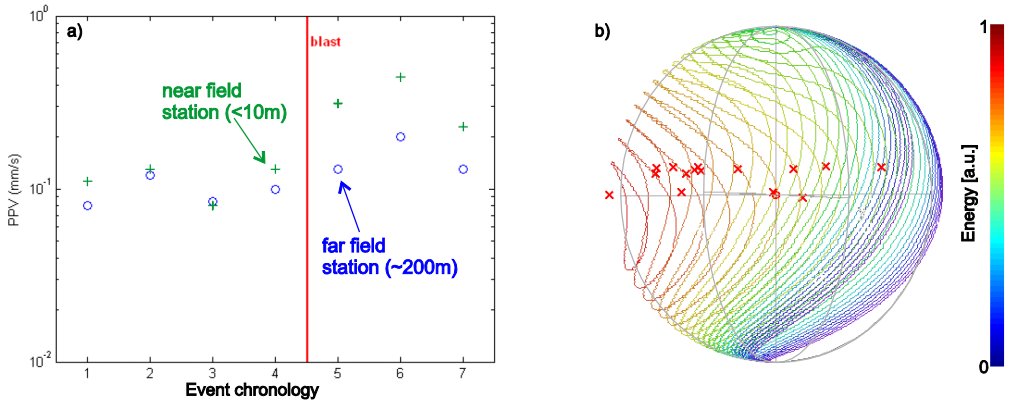

Figure 10: a) PPV change after a blast close to a seismic station (near field) shows local change when comparing the PPV response of a far field station. b) Energy of a blast transmitted through the rock mass projected on a unit sphere and presenting asymmetry. The red crosses indicate seismic station location relative to the blast (center of the sphere). Energy is in normalised arbitrary unit.

rpm produce signals with peak frequency at ~29 Hz and fluctuations ranging from 27.5 Hz to 30.5 Hz (Joseph and Welz, 2011).

An example of rock mass change induced by blasting is presented in Fig. 10a. The peak particle velocity (PPV) record of a station located close to a blast (<10 m) shows a significant increase compared to a

reference station located far from the blast. The two to three times PPV increase for the sensor located close to the blast may indicate an increase in fracture intensity (rock mass damage) close to the source. Another indication of the rock mass state is found when looking on how the energy of a blast is transmitted through the rock mass (Fig. 10b). The asymmetry in the transmitted energy suggests that in this case more energy is transmitted toward the western end of the mine. This is in agreement with independent numerical stress modeling of the mining sequence as well as underground observation suggesting that at the western end of the mine, the rock mass is tight and overstressed, whereas at the eastern end it is damaged and relaxed.

4 CONCLUSIONS

This feasibility study illustrates the potential of new monitoring techniques for rock mass change evaluation. In addition, it suggests new directions for the different methods and their potential shortcomings. Techniques based on time-lapse monitoring (e.g. repeated borehole logging) require extra care during data collection in order to insure measurement repeatability. Also the importance of data integration, not only geomechanics related data but also other activity logs (pump, crushers, moving equipment, blasts), is critical when interpreting broad band seismic data sets.

5 AKNOWLEDGMENTS

This work is funded by an equipment grant from NSERC (National Sciences and Engineering Research Council of Canada), CEMI (Centre for Excellence in Mining Innovation) by the Ontario Ministry of Research and Innovation through the SUMIT (Smart Underground Monitoring and Integrated Technology) research program. The contributions by Vale and its collaborating staff, providing access to the mine and support services, are thankfully acknowledged.

6 REFERENCES

DELALOYE, D., HUTCHINSON, J., DIEDERICHS, M. 2012. Using terrestrial LiDAR for tunnel deformation monitoring in circular tunnels and shafts. Submitted to: European Rock Mechanics Symposium (EUROCK 2012).

JOSEPH, T. G., WELZ, M., 2011. Revisiting ground vibrations due to mining equipment motion. CIM Journal 2 (2).

KAO, H., SHAN, S. J., DRAGERT, H., ROGERS, G., CASSIDY, J. F., and RAMACHANDRAN, K., Aug. 2005. A wide depth distribution of seismic tremors along the northern Cascadia margin. Nature 436, 841-844.

LATO, M., DIEDERICHS, M. S., HUTCHINSON, D. J., Sep. 2010. Bias correction for view-limited LiDAR scanning of rock outcrops for structural characterization. Rock Mech. and Rock Eng. 43 (5), 615–628–628.

MADJDABADI, B. M., VALLEY, B., DUSSEAULT, M. B., KAISER, P. K., 2012 Numerical modeling of strain transfer from rock mass to a fibre optic sensor installed inside a grouted borehole. Submitted to 46th U.S. Rock Mechanics Symposium, Chicago.

PICOZZI, M., MILKEREIT, C., PAROLAI, S., JAECKEL, K.-H., VEIT, I., FISCHER, J., ZSCHAU, J., 2010. GFZ wireless seismic array (GFZ-WISE), a wireless mesh network of seismic sensors: New perspectives for seismic noise array investigations and site monitoring. Sensors 10 (4), 3280–3304.

THÉVENAZ, L., 2010. Brillouin distributed time-domain sensing in optical fibers: state of the art and perspectives. Frontiers of Optoelectronics in China 3 (1), 13–21.

VALLEY, B., MADJDABADI, B. M., KAISER, P. K., DUSSEAULT, M. B., 2012. Monitoring mining-induced rock mass deformation using distributed strain monitoring based on fiber optics. Submitted to: European Rock Mechanics Symposium (EUROCK 2012).